Simulate Wind Loading on RUTE SunTracker

Cooperative Research and Development Final Report

CRADA Number: CRD-23-23755

NREL Technical Contact: Ethan Young

NREL is a national laboratory of the U.S. Department of Energy
Office of Energy Efficiency & Renewable Energy
Operated by the Alliance for Sustainable Energy, LLC

This report is available at no cost from the National Renewable Energy Laboratory (NREL) at www.nrel.gov/publications.

Contract No. DE-AC36-08GO28308

Technical Report
NREL/TP-2C00-92401
December 2024

Simulate Wind Loading on RUTE SunTracker

Cooperative Research and Development Final Report

CRADA Number: CRD-23-23755

NREL Technical Contact: Ethan Young

Suggested Citation
Young, Ethan. 2024. *Simulate Wind Loading on RUTE SunTracker: Cooperative Research and Development Final Report, CRADA Number CRD-23-23755.* Golden, CO: National Renewable Energy Laboratory. NREL/TP-2C00-92401. https://www.nrel.gov/docs/fy25osti/92401.pdf.

NREL is a national laboratory of the U.S. Department of Energy
Office of Energy Efficiency & Renewable Energy
Operated by the Alliance for Sustainable Energy, LLC

This report is available at no cost from the National Renewable Energy Laboratory (NREL) at www.nrel.gov/publications.

Contract No. DE-AC36-08GO28308

Technical Report
NREL/TP-2C00-92401
December 2024

National Renewable Energy Laboratory
15013 Denver West Parkway
Golden, CO 80401
303-275-3000 • www.nrel.gov

NOTICE

This work was authored by the National Renewable Energy Laboratory, operated by Alliance for Sustainable Energy, LLC, for the U.S. Department of Energy (DOE) under Contract No. DE-AC36-08GO28308. Funding provided by U.S. Department of Energy Office of Energy Efficiency and Renewable Energy Solar Energy Technologies Office. The views expressed herein do not necessarily represent the views of the DOE or the U.S. Government.

This report is available at no cost from the National Renewable Energy Laboratory (NREL) at www.nrel.gov/publications.

U.S. Department of Energy (DOE) reports produced after 1991 and a growing number of pre-1991 documents are available free via www.OSTI.gov.

Cover Photos by Dennis Schroeder: (clockwise, left to right) NREL 51934, NREL 45897, NREL 42160, NREL 45891, NREL 48097, NREL 46526.

NREL prints on paper that contains recycled content.

Cooperative Research and Development Final Report

Report Date: December 4, 2024

In accordance with requirements set forth in the terms of the CRADA agreement, this document is the final CRADA report, including a list of subject inventions, to be forwarded to the DOE Office of Scientific and Technical Information as part of the commitment to the public to demonstrate results of federally funded research.

Parties to the Agreement: Rute Foundation Systems

CRADA Number: CRD-23-23755

CRADA Title: Simulate Wind Loading on RUTE SunTracker

Responsible Technical Contact at Alliance/National Renewable Energy Laboratory (NREL):

Ethan Young | Ethan.Young@nrel.gov

Name and Email Address of POC at Company:

Doug Krause | kraused@rutefoundations.com

Sponsoring DOE Program Office:

Office of Energy Efficiency and Renewable Energy (EERE), Solar Energy Technologies Office (SETO)

Joint Work Statement Funding Table showing DOE commitment:

Estimated Costs	Contractor In-Kind	Totals
Year 1	$75,000	$75,000.00
TOTALS	$75,000	$75,000.00

Executive Summary of CRADA Work:

RUTE produces and delivers efficient, sustainable structural foundation systems for the wind and solar industries, instrumental in the effort to lower the cost of clean electricity and reduce CO2. RUTE's SunTracker is a high clearance agrivoltaics solar array. The system uses raised cables, providing support with less materials and cost. These cables can provide tracking for increased energy generation and greater revenue, allowing the land beneath to be used for other means simultaneously. RUTE provided data files that NREL will use to perform computational fluid dynamics (CFD) simulations to characterize and predict wind loading on the 6x6 RUTE SunTracker photovoltaic (PV) array. Varying both the panel orientations and wind speeds provides information on how the array can manage a variety of weather conditions. These results, in turn, inform RUTE's design and construction of these arrays.

CRADA benefit to DOE, Participant, and US Taxpayer:

- adds new capability to the laboratory's core competencies.
- enhances the laboratory's core competencies,
- uses the laboratory's core competencies and/or
- enhances U.S. competitiveness by utilizing DOE developed intellectual property and/or capabilities.

Summary of Research Results:

The intent of this project was to investigate and report on the effects of wind loading on the RUTE SunTracker photovoltaic (PV) array in a variety of orientations and wind speeds utilizing CFD simulations. RUTE will utilize these results to design and construct these arrays. Below is a summary of the tasks outlined in the Statement of Work and the corresponding results.

Task 1: The Contractor will build a 3D model for the geometric representation of Photovoltaics (PV) system in wind simulations. The Participant will provide 3D CAD model files or a suitably detailed description and assist with questions relevant to the construction of this model.

1.1 Task 1

In task 1, RUTE provided 3D CAD model files and detailed descriptions of the SunTracker array's geometric and layout data. NREL utilized this information to build a 3D model for the geometric representation of the PV system in wind simulations using our in-house software PVade, an open-source Python package for simulating the effect of wind and aeroelastic effects on PV systems [1]. Utilizing this initial model, NREL ran simulations depicting surface pressure and wind velocity representing a single wind speed and panel orientation and post-processed a variety of different results for the RUTE team's presentation at the Solar Prize Demo Day.

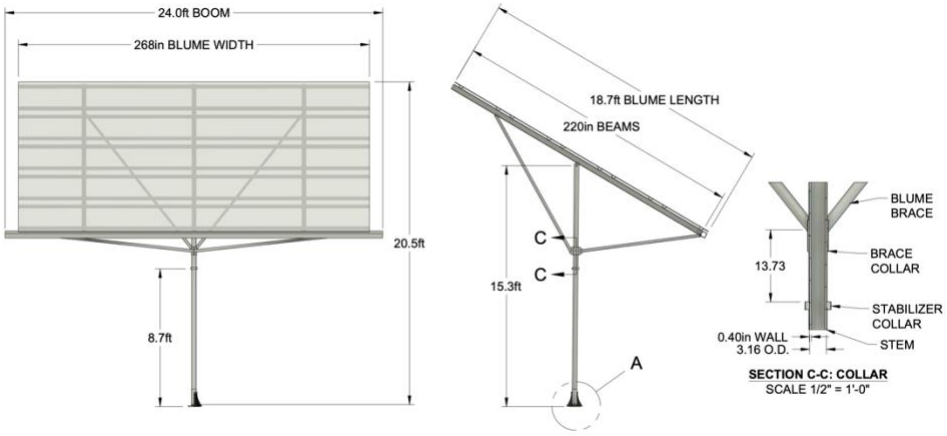

Figure 1: An example of the system descriptions provided by RUTE. All studies presented in this report use the dimensions shown above and provided in the remainder of the CAD models (not shown).

We started with a small, 3x3 array to both demonstrate that the initial system definitions were being implemented correctly and for the sake of being able to rapidly produce a simulation in time for the Solar Prize Demo Day. The specific files that NREL delivered to RUTE included: PowerPoint slides defining the simulation setup and key parameters, e.g., wind speed; animated videos of flow results; plots of differential surface pressure over time; and the complete set of CSV files used to produce those plots prior to Solar Prize Demo Day. A snapshot of the movie used in the Demo Day presentation is shown in Figure 2.

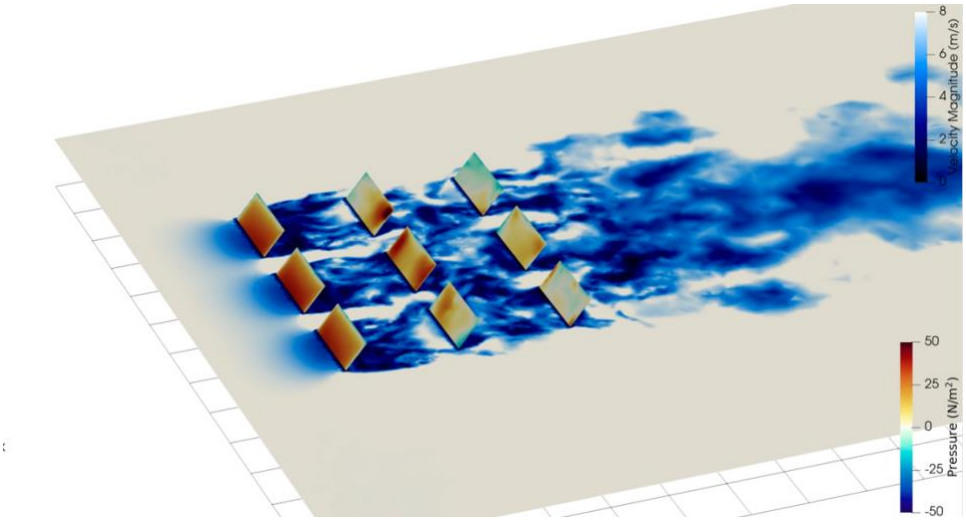

Figure 2: A Snapshot of a simulation of flow through a 3x3 array of panels, here, the wind speed at the height of the vertical panel centers is 17.9 miles per hour (mph). The ground-parallel plane illustrates the velocity magnitude of the surrounding fluid (darker blue is faster) and the pressures on the panel surfaces are colored between blue and orange where blue is a negative pressure relative to ambient and orange is positive.

This snapshot shows how wind moving from left to right generates a strong force on the surface of the leading edge (left-hand side). Panels and a strong mixing effect behind them (right-hand side) Panels in these downstream rows experience a much more turbulent flow condition manifested as the strongly spatially varying surface forces. The snapshot in Figure 2 represents an instantaneous moment from a larger, time-varying simulation, which is plotted in its entirety in Figure 3.

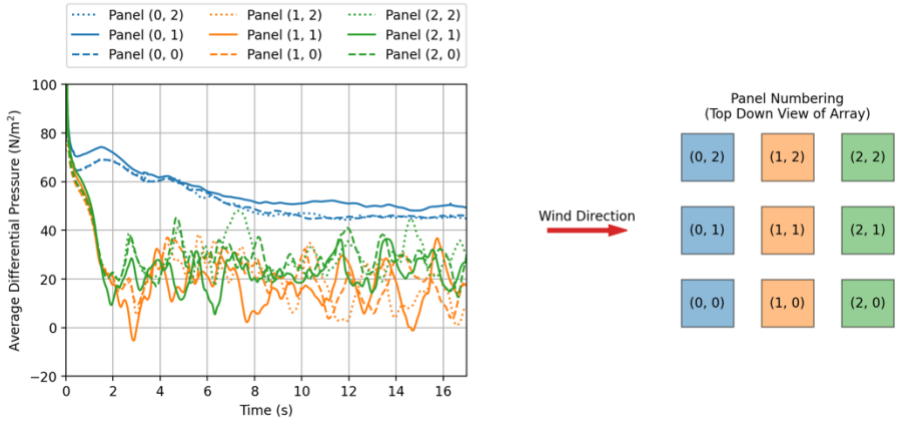

Figure 3: (left) the average differential pressure generated between the top and bottom surface of each panel as a function of time, (right) the wind direction is indicated by the arrow and the panels are numbered and colored according to their position in this top-down view.

Figure 3 shows the average differential pressure as a function of time for all panels in our 3x3 array. The leading-edge panels are colored blue and exhibit a higher mean force and less oscillation due to experiencing a non-waked inflow condition. The orange and green panels, which reside in blue's wake, see significantly less average force but much more variability in the surface pressures, as evident by the wider range of forces in their respective time series curves.

Task 2: The Contractor will run computational fluid dynamics (CFD) simulations of various panel orientations and wind conditions. The Participant will provide a range of direction and wind condition cases based on interaction with the Contractor.

1.2

RUTE provided feedback to NREL on the Solar Prize Demo Day results to be incorporated into NREL's simulation work. These changes included increasing the number of panels from 9 to 25, that is, replacing the 3x3 array with a 5x5 array, and increasing the maximum wind speed tested to ~70 mph. Additionally, we produced numerous changes to the postprocessing workflow that allowed us to analyze our results. Importantly, this included saving the more intuitive total integrated force per each panel as a function of time rather than relying solely on the differential pressure force. NREL ran additional simulations, providing a range of direction and wind condition cases based on direction provided by RUTE. Before presenting these new results, we must first define another labeling convention to help with interpretation of the more extensive analysis performed in tasks 2 and 3.

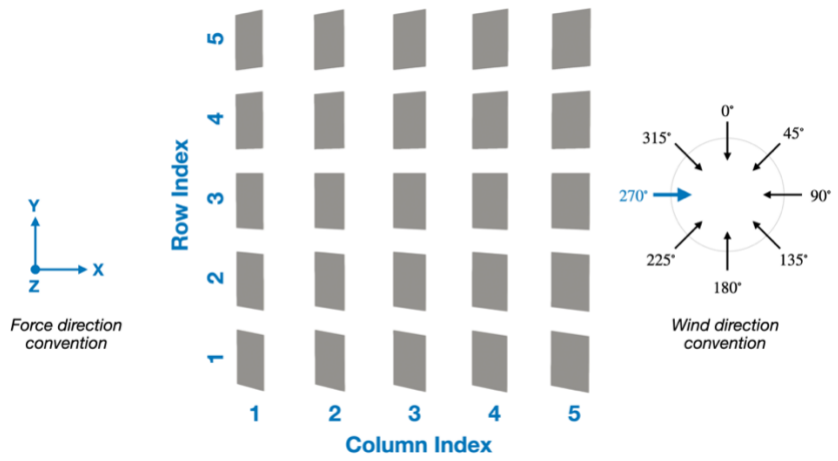

Figure 4: The conventions used in the remainder of this report, from left to right, (1) forces on panels are reported in the x- and y-directions shown, (2) a top-down view of the 5x5 panel array, where column numbers increase along the +x-axis and row numbers increase along the +y-axis, and (3) the specification of the wind inflow direction, where a 0° wind flows in the -y-direction, a 270° wind flows in the +x-direction, and so on, as indicated by the wind direction arrows.

Using this setup, we simulated the 8 different wind directions shown in Figure 4, that is, 45° intervals, generating a final list of inflow directions [0, 45, 90, 135, 180, 225, 270, 315] °. We simulated two different wind speeds, 16 and 32 m/s, or 35.8 and 71.6 miles/hour (mph), respectively, to capture both the upper limit for insurability concerns as well as a lower wind speed for verifying the relationship between wind speed and load. Finally, we swept over panel tilt angles of 22, 45, and 90°, where the panel angle is defined as shown in Figure 5.

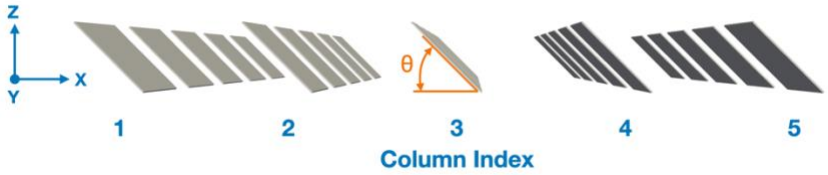

Figure 5: The convention used for panel tilt angle, θ, relative to the ground, 22° corresponds to a relatively flat orientation (roughly parallel to ground), 90° orients the panels normal to the x-axis, and 45° (shown here) corresponds to a typical position at the beginning or end of the day.

Although the panel angle of 90° may be well outside the norm for a tilt angle that maximizes capturing solar irradiance or energy production, it was a desirable test from the point of view of understanding a worst-case wind loading scenario in which the panels present their maximum possible surface area to the oncoming wind. With the idea of this worst-case orientation in mind, we present the results of the 35.8 mph, 270° wind loading with the panels oriented at 90° in Figure 6.

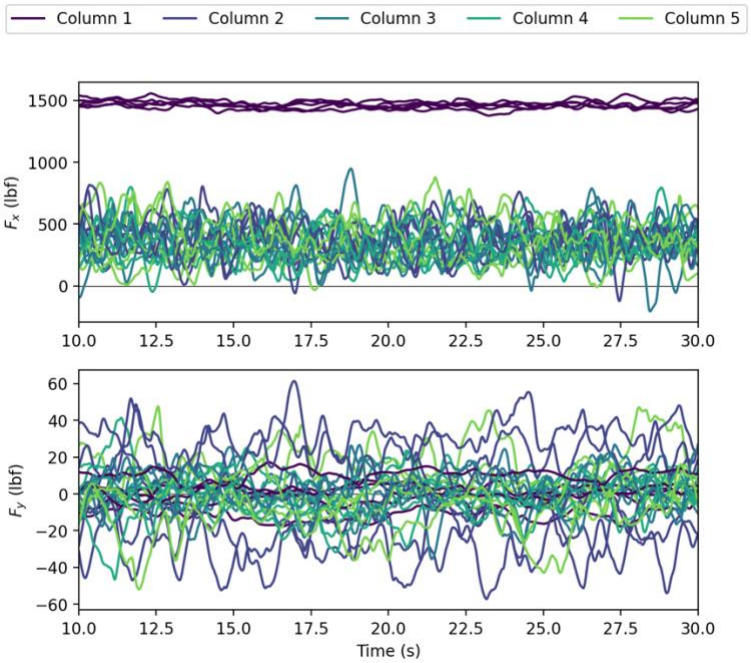

Figure 6: Time series of the total force in the x-direction (top) and y-direction (bottom) on each panel in the array under 35.8 mph, 270° wind at a tilt angle of 90°, colors indicate panels in each column number, that is, column 1 corresponds to the 5 "leading" edge panels of the array and columns 2-5 are somewhat shielded by their upstream neighbor(s).

In Figure 6, we see that the total force is dominated by the x-component (aligned with the direction of the flow) and that there is a clear delineation between the leading-edge panels in column 1 and those in columns 2-5 that exist in the wake of at least one upstream panel. The x-component of force also shows a clear positive bias, that is, all panels experience a positive average force (along the +x-direction) with some degree of oscillation around that value. Less oscillation is observed in column 1, likely because it alone experiences an un-waked inflow due to residing farthest upstream. Note that at this point we do not make any attempt to distinguish between different spanwise rows normal to this flow direction in the time series and reserve that for the more statistical approach that follows in Section 1.3, where each panel will be reported as a mean and fluctuating load component. We will first examine the effect of increasing the wind speed from 35.8 to 71.6 mph in Figure 7.

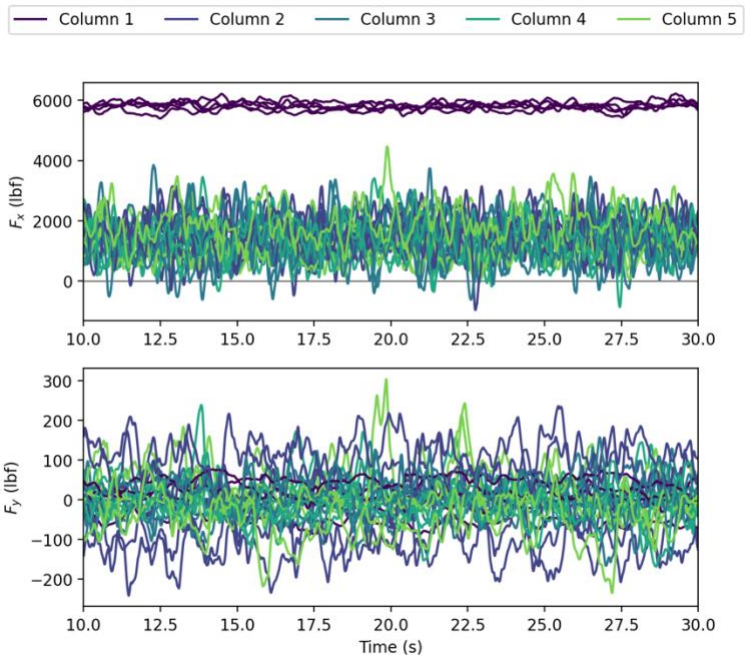

Figure 7: Time series of the total force in the x-direction (top) and y-direction (bottom) on each panel in the array under 71.6 mph, 270° wind at a tilt angle of 90°, colors indicate panels in each column number.

Intuitively, Figure 7 illustrates clearly that larger wind speeds are associated with universally larger loads on panels. When subjected to 71.6 mph wind, the average load for the panels on the leading edge, i.e., column 1, is ~5811 pounds force (lbf), where the average load for the 35.8 mph wind was 1463 lbf. This relationship shows the expected scaling, where load is a function of wind speed squared, or $F \propto u^2$, as doubling the wind speed from 35.8 to 71.6 mph resulted in an $4\times$ increase in the average x-component of load experienced in the panels of column 1.

For the Task 2 deliverable, NREL provided access to the database of simulation results provided via OneDrive, a compilation of cases in the form of the complete set of CSV files used to produce the plots in this report, and a post-processing notebook used to run statistical analysis and produce figures.

Task 3: The Contractor will analyze selected simulations including time- and spatially varying loads and inter-panel interactions at different positions in the array.

1.3

In this task, NREL performed a much deeper dive into the outcomes from the parameter sweep outlined in Section 1.2 and analyzed time- and spatially varying loads and inter-panel interactions at different positions in the array. We include this analysis in the final report, which summarizes the wind load parameters on the SunTracker array, with particular attention paid to the integrated forces defined in Section 1.2. In addition to this report, we provide technical feedback to improve the PV technology based on the simulated results and provided suggestions for future simulations including aerodynamic stability analyses and guidance on future experimental setups.

As seen in Section 1.2, the forces and dynamics generated by the cases with 71.6 mph inflow velocity far exceed those generated by the 35.8 mph cases, and thus, for the sake of informing a safe and reliable system design, we devote the remainder of this report to presenting those results. We begin by revisiting the 71.6 mph case presented in Figure 7, where the wind direction was 270° and the tilt angle was 90°. However, rather than looking at the time series data, we calculate the mean and standard deviation of each time series curve and label each panel in its appropriate spatial position with both the mean and oscillating (standard deviation) component. The results of these analyses are shown in Figure 8.

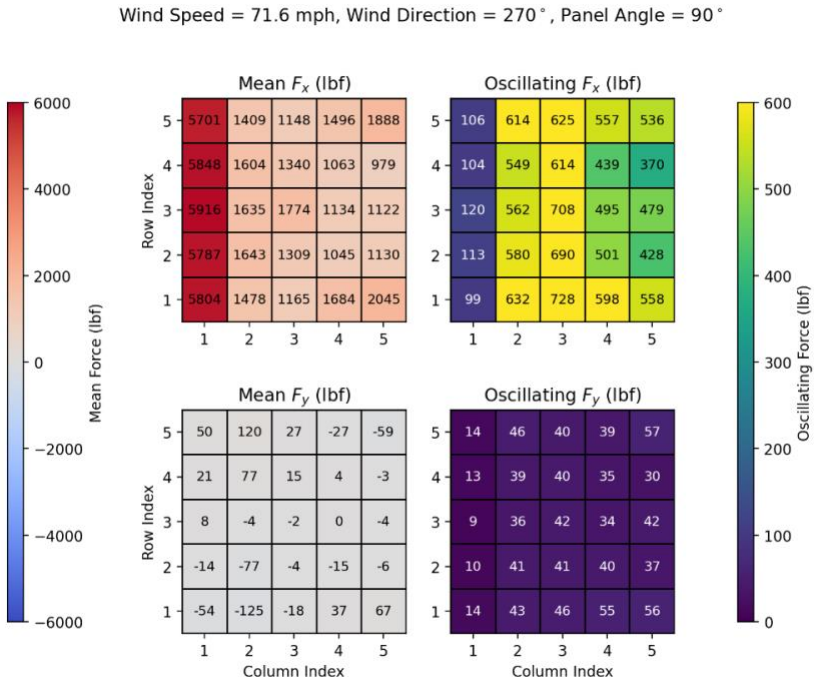

Figure 8: The load statistics obtained from the CFD simulations spatially arranged into rows and columns corresponding to a top-down view of the 5x5 array; the two left-hand plots correspond to the mean load calculated from the x- and y-component of force per each panel, and the two right-hand plots correspond to the oscillating load calculated from the x- and y-component of force per each panel, note the separate color bars for mean and oscillating forces.

Compared to Figure 7, Figure 8 reveals the same strong mean component in the force in the x-direction in column 1 due to the unobstructed flow field it is subjected to. However, Figure 8 also offers a way to clearly separate effects between both streamwise columns and spanwise rows. It is evident from looking at the mean x-component of force that the panels in column 2 experience a relatively large loading relative to the other panels in columns 2-5 and that the perimeter panels (e.g., row 1, column 4, and row 5, column 5) also experience larger-than-average forces. Looking at the oscillating component of the x-force, it is clear that column 1 experiences a much steadier flow versus columns 2-5, which each experience a waked flow state due to their upstream neighbor(s). It is interesting that this oscillating load seems to experience a peak at column 3, then be reduced in columns 4-5, which suggests that sufficient fixation methods to resist these interior forces be included in the system design. Regarding the components of force in the y-direction, it is evident that 270° wind creates a scenario where most of the total force is aligned with the x-axis, with near-zero values for the mean y-force and an order of magnitude less oscillating force. We present two additional cases focused on isolating the effect of panel tilt angle in Figures 9 and 10.

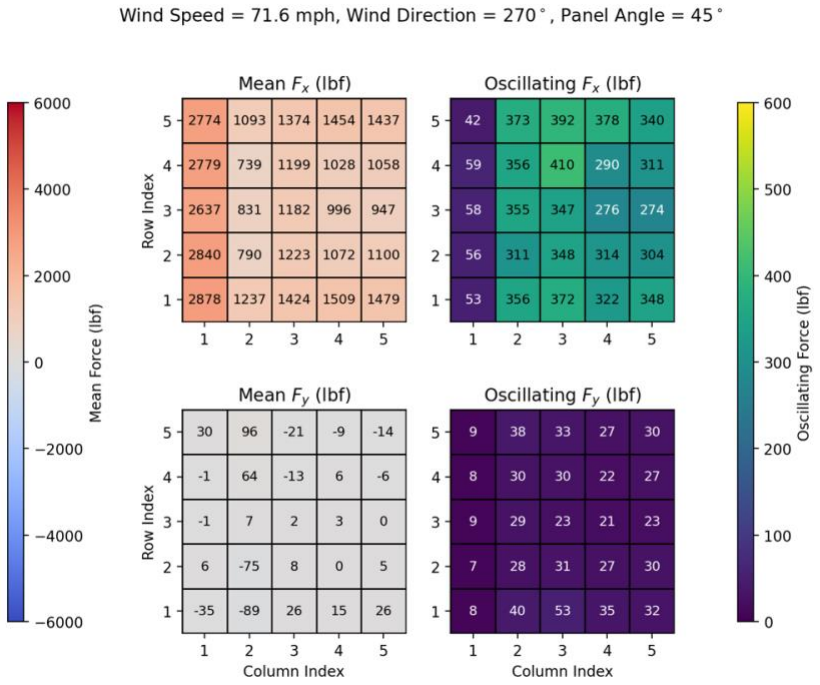

Figure 9: Orienting panels at 45° for the same 71.6 mph, 270° wind results in generally lower-magnitude forces throughout the array, however, interior panels seem to be somewhat more "protected" versus the 90° tilt angle as evidenced by the smaller mean force in column 2, while the effect of stronger forces on perimeter rows is slightly less pronounced.

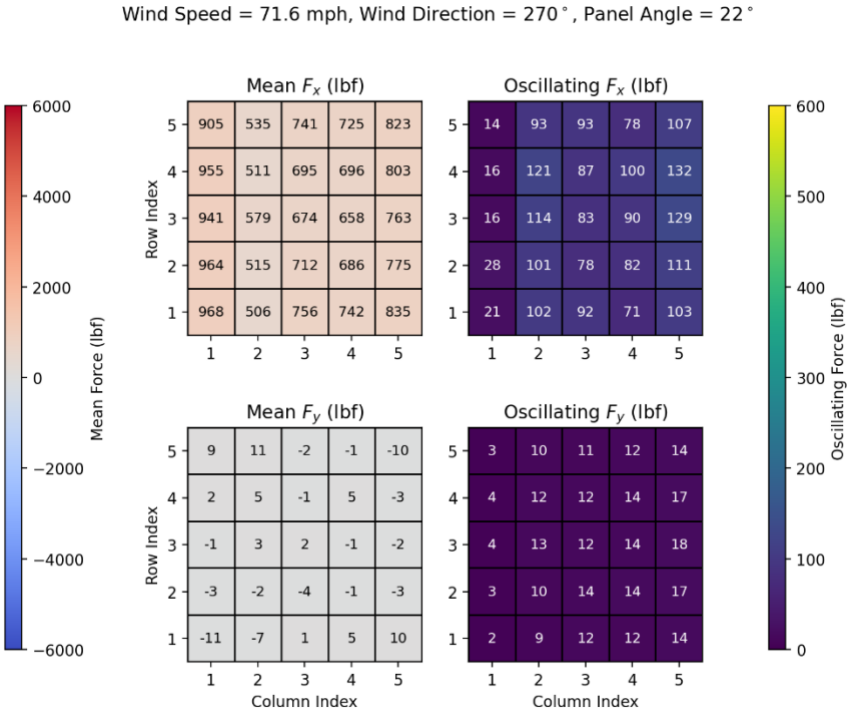

Figure 10: Orienting panels at 22° for the same 71.6 mph, 270° wind again reduces the total magnitude of force experienced by panels in the array and generates a more uniform distribution of force, with a less pronounced perimeter effect and a less dramatic drop-off in the forces observed in columns 1 and 2.

As seen in Figures 9 and 10, the effect of tilt angle is, largely, a reduction in the total magnitude of stress, a less pronounced difference between perimeter and interior rows, and a reduction in the sharp change in force that occurs within columns 1, 2, and 3. Before turning attention to varying wind directions, let us look at the difference between positive and negative tilt angle orientation; that is, when keeping the panels fixed at 45° and reversing the direction of flow, i.e., changing the wind direction to 90°. The relevant statistics for this case are summarized in Figure 11.

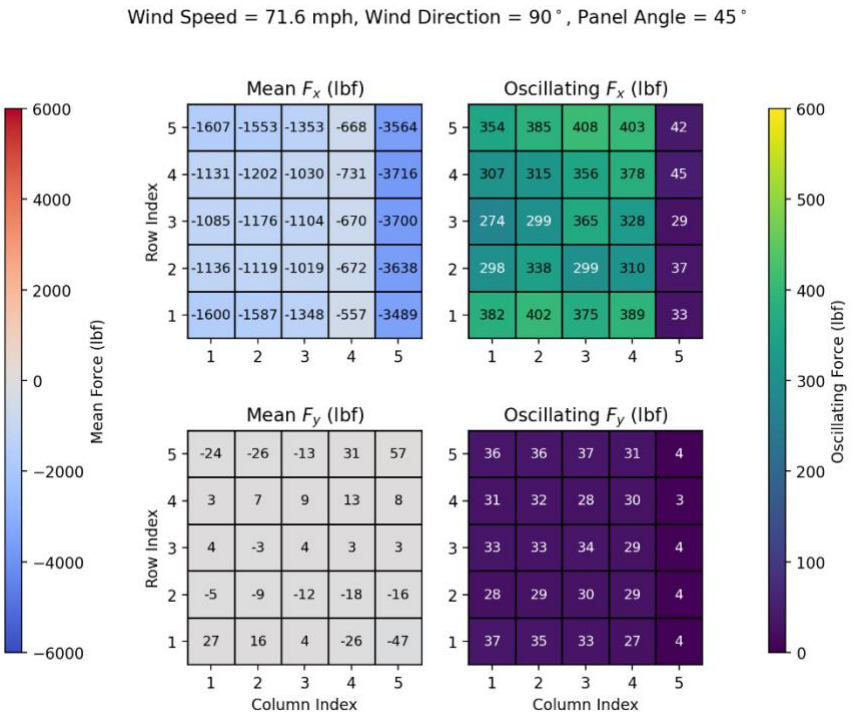

Figure 11: The opposite-wind-direction counterpart to Figure 9, note the stronger magnitude x-component of force in what is now the leading column, column 5, and the more pronounced shielding of its immediate downstream neighbor, column 4, compared to the magnitudes seen in Figure 9.

Figure 11 reveals an interesting behavior: that there is a clear difference between the forces generated when wind impacts a +45° versus a -45° panel[1]. Namely, the leading-column force experiences a larger mean load when the wind direction is reversed, and the immediate downstream neighboring column appears to be more shielded from the wind. These dynamics are certainly interesting and merit more study in the future. However, since we are primarily concerned with informing a system design which can withstand the highest loads, we will finish the report looking at tilt angles of 90°, that seem to generate the highest loads in all cases due to their orientation creating the largest cross-sectional surface area normal to the flow. Figures 12 and 13 illustrate the effect of 71.6 m/s flow at 315° and 45°, respectively, with a tilt angle of 90°.

1 Here we imagine keeping the wind direction fixed at 270° and "flipping" the tilt angle such that the leading edge of the panel is closer to the ground compared to the trailing edge, or effectively rotating the 90° wind direction, +45° tilt angle case to match the wind direction of the 270° case.

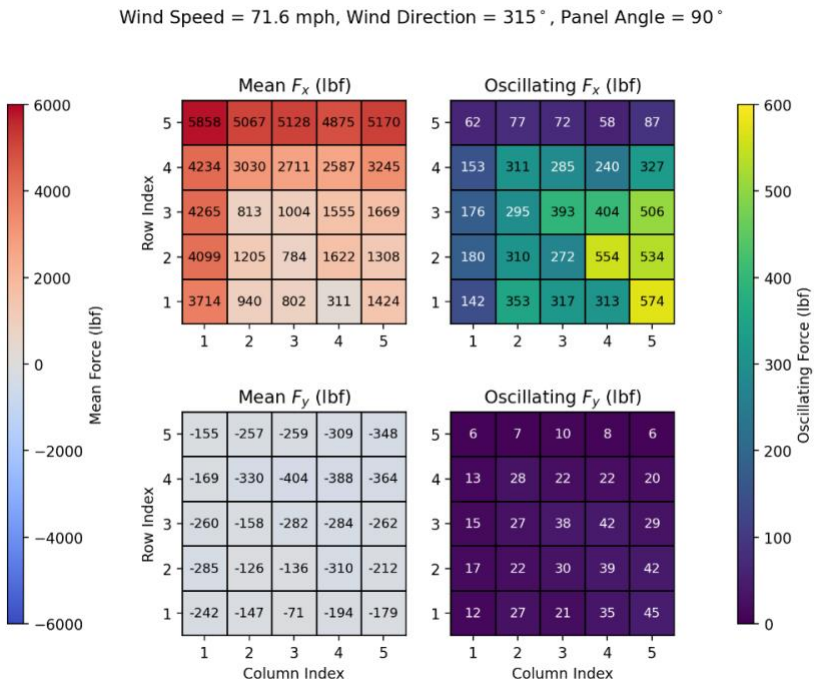

Figure 12: A wind direction of 315° places the panel at row 5, column 1 at the extreme leading point, and thus, it experiences the largest force, the remaining panels in row 5 and column 1 experience partial shielding and are less severely loaded as a result. Note the strong component of oscillating force manifested in panels aligned with the flow direction.

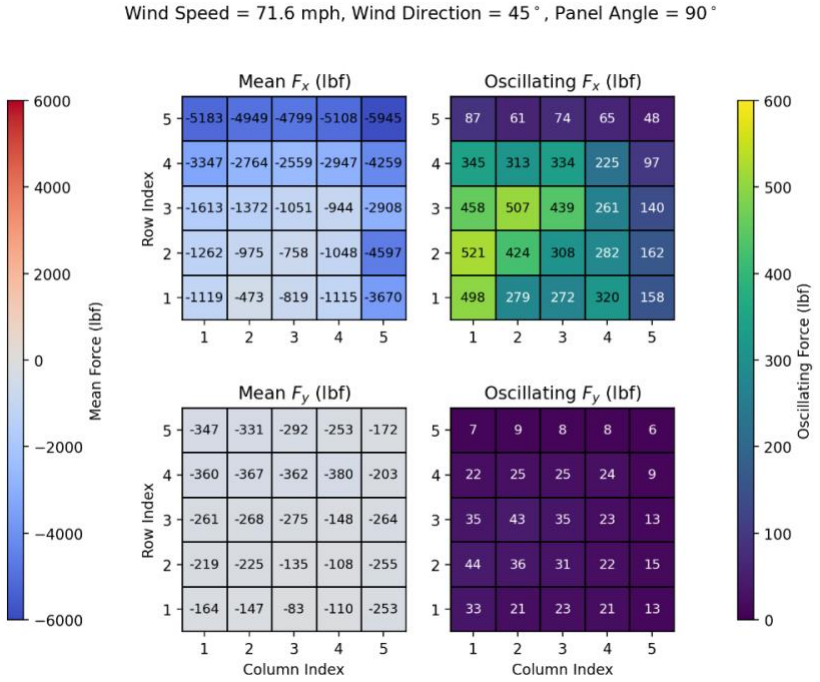

Figure 13: A wind direction of 45° places the panel at row 5, column 5 at the extreme leading point, and thus, it experiences the largest force. As in Figure 12, note the strong perimeter effect, partial shading, and flow-aligned manifestation of strong force oscillations.

The diagonally aligned wind directions produce another set of interesting results with interesting array-dependent interactions. In both cases, the most upstream corner panel experiences the maximum mean loading, and in both cases, the magnitude of that mean loading is approximately equal to the loading obtained with the flow direction that was normal to the panel surface (i.e., 270° and 90°). The presence of the strong oscillating component along the diagonal path of the wind direction hints at the possibility of effects deeper into the array resulting from an asymmetric waked loading condition, but a finer parameterization of wind directions and a larger simulated array would be necessary to see in what conditions this effect arises.

The complete list of results and simulations generated in tasks 2 and 3 includes 2 wind speeds, 8 wind directions, and 3 panel tilt angles for a total of 48 large 3D simulations. For the sake of brevity, we focused on presenting the most severe loading conditions in this report. However, the complete set of all 48 3D simulations along with the time-varying CSV files containing integrated load outputs were shared with RUTE along with this report upon the completion of this project. Our recommendations for the RUTE system design are largely implied by the preceding discussion, but a few points bear reiterating here. The largest load on panel surfaces peaks at around 6000 lbf and is associated with a tilt angle of 90° and a wind speed of 71.6 mph. Interestingly, this load scenario can arise in multiple different wind directions, both 270° and 90° but also in much more localized instances at the corners of the 5x5 array when the wind direction was 315° and 45° (and 225° and 135°, not shown here). These corner panels are in the unique position of experiencing the largest loads in multiple wind conditions and (potentially) having the fewest connections to neighbors via the rotator and stabilizing cables. We recommend that the total amount of cable-provided fixation exceed this maximal load by a large safety margin and across the range of different inflow directions discussed above. Note that although the components of force in the y-direction are consistently small under the orientation assumptions considered here, revolving the panels within the array such that the leading/trailing edges are no longer aligned with the y-axis would lead to a corresponding shift of the location of maximal loads. By symmetry, we expect the behavior of these loads to be much the same as what can be observed with the current set of results and the appropriate wind direction, but further study should be done to ensure that there are no unexpected effects at particularly dynamic locations in the overall parameter space. Additionally, future work should focus on characterizing the effect of panel displacements on these loads, where linked panels can provide an accumulated tension by the nature of the rotator and stabilizing cable connections. We attempted to implement a greatly simplified version of this dynamic effect in the current study but found that the multi-point constraint required to apply these loads was beyond what could be achieved in this project.

2 CRADA Artifacts

Subject Inventions Listing:

None.

ROI #:

None

Products, Applications, and Technology Transfer Activities

No products, applications, or tech transfer activities to report. However, a small portion of the results from Section 1.1, Figures 2 and 3, was included in a DuraMAT Network meeting:

Young, E., Arsalane, W., Stanislawski, B., He, X., Ivanov, C., Dana, S., & Deceglie, M., "A simulation framework for managing wind-driven loading on PV systems", DuraMAT Network Meeting, January 22, 2024.

References

1. Young, E., Arsalane, W., Stanislawski, B., He, X., Ivanov, C., Dana, S., & Deceglie, M. (2023). PVade (PV Aerodynamic Design Engineering) [SWR-23-49] [Computer software]. https://doi.org/10.11578/dc.20231208.1